NJC

New Journal of Chemistry

An international journal of the chemical sciences

www.rsc.org/njc

Volume 33 | Number 8 | August 2009 | Pages 1621–1792

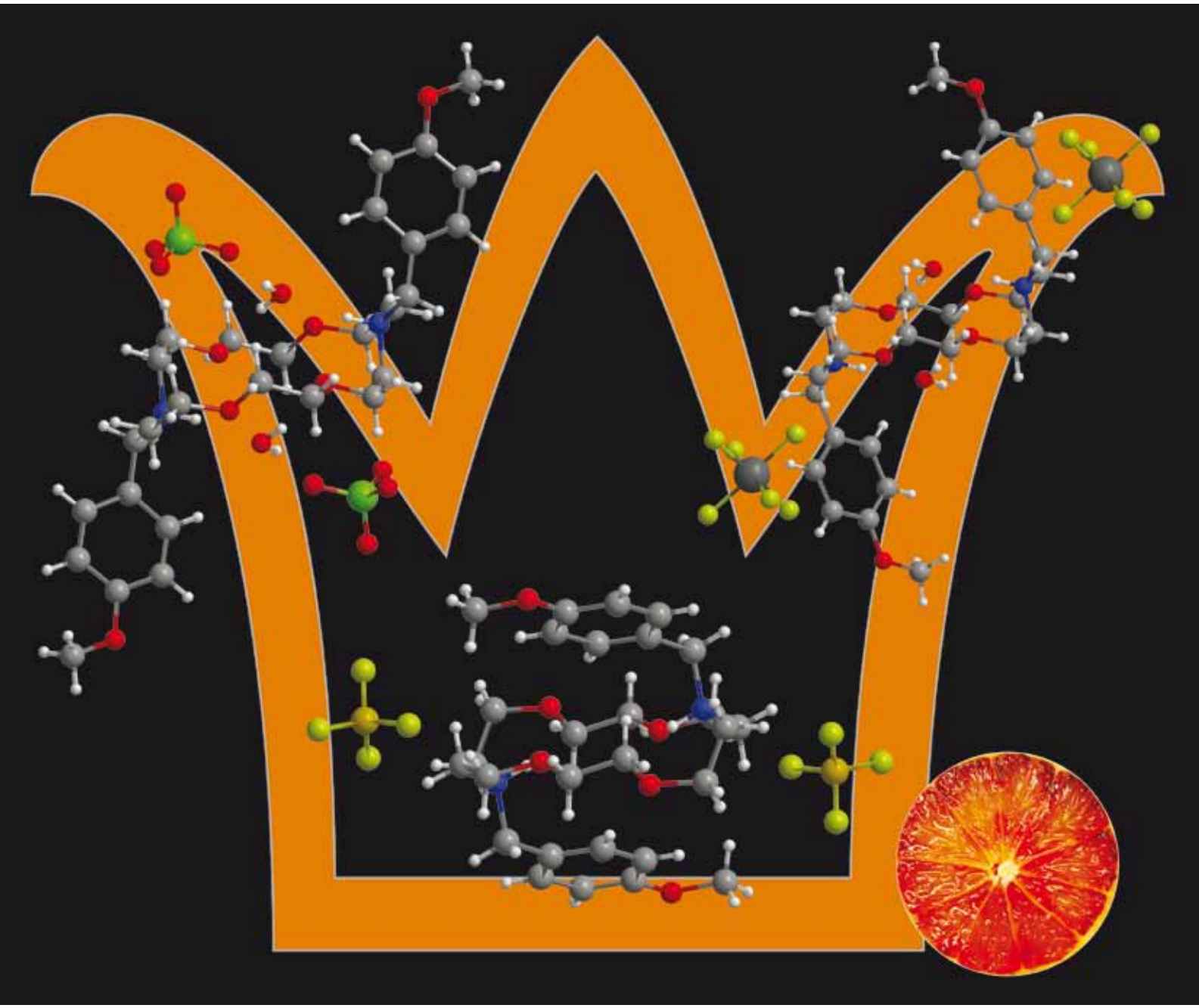

ISSN 1144-0546

RSC Publishing

PAPER
Marina S. Fonari *et al.*
Conformational mobility of 7,16-bis(4-methoxybenzyl)-1,4,10,13-tetraoxa-7,16-diazacyclooctadecane in molecular and proton-transfer complexes

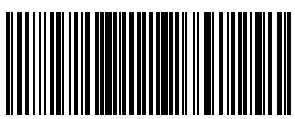

1144-0546(2009)33:8;1-W

Conformational mobility of 7,16-bis(4-methoxybenzyl)-1,4,10,13-tetraoxa-7,16-diazacyclooctadecane in molecular and proton-transfer complexes: X-ray and DFT studies†

Marina S. Fonari,*[a] Eduard V. Ganin,[b] Yurii M. Chumakov,[a] Mark M. Botoshansky,[c] Kinga Suwinska,[d] Stepan S. Basok[e] and Yurii A. Simonov[a]

Received (in Victoria, Australia) 12th February 2009, Accepted 22nd April 2009
First published as an Advance Article on the web 28th May 2009
DOI: 10.1039/b902953b

For the first time the bibracchial-crown ether 7,16-bis(4-methoxybenzyl)-1,4,10,13-tetraoxa-7,16-diazacyclooctadecane (**1**) and its molecular and proton-transfer complexes were isolated and characterized by X-ray single-crystal diffraction. Hydrogen bonding between the neutral molecules is present in the binary complex **1**·$(H_2NCS)_2$ (**3**) giving rise to a tape structure. The proton migration from an inorganic acid to a macrocyclic molecule results in doubly protonated cations $(\mathbf{1}\text{-}H_2)^{2+}$ and $(\mathbf{2}\text{-}H_2)^{2+}$ (where **2** is the parent 7,16-dibenzyl-1,4,10,13-tetraoxo-7,16-diazacyclooctadecane) giving rise to the ionic complexes $(\mathbf{1}\text{-}H_2)\cdot[ClO_4]_2\cdot 2H_2O$ (**4**), $(\mathbf{1}\text{-}H_2)\cdot[NbF_6]_2\cdot 2H_2O$ (**5**), $(\mathbf{1}\text{-}H_2)\cdot[TaF_6]_2\cdot 2H_2O$ (**6**), $(\mathbf{1}\text{-}H_2)\cdot[BF_4]_2$ (**7**) and $(\mathbf{2}\text{-}H_2)\cdot[ClO_4]_2\cdot 2H_2O$ (**8**) sustained by a system of charge-assisted hydrogen bonding. The macrocyclic entities in **1–8** differ by the conformation of the crown ring and the arrangement of the pendant arms. To rationalize the different conformations of **1** in comparison with the relative compounds based on **2**, the theoretical quantum chemical calculations on the DFT (B3LYP) level were performed. The contribution of the methoxy group that provides the C–H···O(OCH_3) hydrogen bonding to the overall system of intermolecular interactions has been estimated by comparison with the complexes based on **2**.

Introduction

The crown ether family of macrocyclic compounds has attracted a huge amount of interest since its discovery in 1967,[1,2] especially in the fields of host–guest and coordination chemistry. The metal ion complexing abilities of crown ethers can be improved significantly by their functionalization with ligating side arms that enhance the cation selectivity and transport through liquid membranes.[3] The C- or N-pivot, bibracchial (two arms) lariat ethers (BiBLEs)[4,5] were modeled on valinomycin complexation and designed to be flexible and dynamic when unbound and enveloping when a guest is complexed.[6] The historically first synthesized *N*,*N*′-dibenzyl-1,7,10,16-tetraoxo-4,13-diazacyclooctadecane (*N*,*N*′-dibenzyl-diaza-18-crown-6, **2**)[4,5,7] has been studied in detail, and it has manifested itself as a good complexing agent for a wide range of metals, both inside the cavity acting in its neutral form and in an outer-sphere coordination. Evans and co-workers[8] have indicated that the alkaline and lighter lanthanoid species (La–Sm) tend to form inclusion-type compounds with a metal salt incorporated into the macrocyclic cavity. It results in different crown conformations: an asymmetric 'basket-like' shape with two phenyl substituents situated on the same side of the macrocyclic cavity as in the cases of NaI·**2**[8] and $Ln(NCS)_3$·**2** (Ln = La, Nd, Eu),[9] a T-shaped arrangement of two phenyl substituents in the complex $AgPF_6$·**2**,[10] and a more symmetric conformation with benzyl arms splayed up from the both sides of the macrocyclic ring in *catena*-((μ_2-isothiocyanato-*N*,*S*)-(μ_2-thiocyanato-*N*,*S*)-bis(**2**)-di-potassium).[5] In contrast, protonation of the aza-crown ether inhibits inclusion of the lanthanoid species, affording complex metal anion species interspersed between the network of crown dications.[8] In a similar way, the recently reported metal-free structures of $(\mathbf{2}\text{-}H_2)\cdot[BF_4]_2\cdot H_2O$[11] and $(\mathbf{2}\text{-}H_2)\cdot I_8$[12] as well as $[Na\cdot N,N'$-dipyridyl-bis-aza-18C6$]_2[(H^+)_2 N,N'$-dipyridyl-bis-aza-18C6$][ClO_4]\cdot 2H_2O$[13] revealed unusual C–H···π interactions between the phenyl substituents and two macrocyclic methylene protons that effectively anchor the ring into the folded conformation and inhibit flexing, typical for macrocycles of this type. Extended studies were devoted to the modification of

[a] *Institute of Applied Physics, Academy of Sciences of Moldova, Academy str., 5 MD2028 Chisinau R., Moldova. E-mail: fonari.xray@phys.asm.md; Fax: +373 22 72 58 87; Tel: +373 22 73 81 54*
[b] *Odessa State Environmental University of Ministry of Education and Science of Ukraine, Lvovskaya str.15, 65016 Odessa, Ukraine. E-mail: edganin@yahoo.com*
[c] *Schulich Faculty of Chemistry, Technion-Israel Institute of Technology, Technion City, 32000 Haifa, Israel. E-mail: botoshan@tx.technion.ac.il*
[d] *Institute of Physical Chemistry Polish Academy of Science, Kasprzaka, 44/52, Warsaw, Poland. E-mail: kinga@ichf.edu.pl*
[e] *A.V. Bogatsky Physico-Chemical Institute, National Academy of Science of Ukraine, Lustdorfskaya doroga 86, 650080 Odessa, Ukraine*

† Electronic supplementary information (ESI) available: Overlapping diagram (Fig. S1) for **1** and **2** in the relative complexes, table of torsion angles (Table S1) along with the macrocyclic framework of **2** in the complexes parent to those discussed herein. The coordinates for all optimized conformers are available from the authors. CCDC reference numbers 717101–717107. For ESI and crystallographic data in CIF or other electronic format see DOI: 10.1039/b902953b

the pendant side arm by the introduction of the fluorescent or redox switched moieties in the molecule.[14] Lariat ethers appear to be good candidates to analyze the cation–π interactions with the participation of the pendant arm. The fruitful conclusion made by Gokel's group that the arenes should be placed two carbons from the macrocyclic nitrogen rather than one permitted them to prove the contribution of one and two arms to the metal complexation.[15] Special attention has been drawn to the substituents mimicking the function of the four amino acids possessing aromatic side chains capable of complexing alkali metal cations, phenylalanine (benzene), tyrosine (phenol), tryptophan (indole), as these aromatic residues are generally regarded as π-donors, and histidine, (imidazole) as a σ-donor.

For decades, the high flexibility of crown ethers (CEs) has impeded their conformational analysis. However, nowadays we are witnesses of the growing number of calculated approaches for analyzing the conformational mobility of CEs in general and lariat-crown ethers (LCEs) in particular. Theoretically, different conformers of CEs can be obtained through a conformational search with molecular dynamics (MD) or molecular mechanics (MM) techniques, while the actual conformer(s) may be retrieved from the Cambridge Structural Database (CSD) when their crystal structures are known. The latter provides a good starting point for a conformational search. For example, Reedijk *et al.*[16] used the computational facilities (MM3, PM3) to estimate the conformational and electronic properties of N,S,O-mixed donor CEs in nucleophilic coupling of their secondary nitrogen atoms to an epoxide. The conformational analysis of *N*-tosyl-substituted diaza-crown ethers theoretically studied by empirical and semi-empirical methods using MSI/DISCOVER97 (ESFF force field) and MOPAC (PM3) permitted the authors to estimate the preferred conformations.[17] C-pivot LCEs were the subject of the DFT calculations by the Chinese group to estimate the side arm remote controlling effect.[18] Through the cooperation of the crown ring and the side arm the LCEs often exhibit different cation-binding properties when compared with their parent CEs. Because the functional groups of side arm LCEs are key components in the formation of metal–CE complexes and in molecular recognition, detailed information about the conformational energies of LCE is important for the understanding of the binding affinities of the crownophanes with guest molecules and for the design of artificial host molecules. Platas-Iglesias and co-workers have carried out a systematic investigation of the electronic structure and changes in conformations on lariat ethers in the complexes, starting from the X-ray data using DFT facilities.[19]

The aza-crown ethers bearing the phenolic side arms are very attractive targets and their synthesis has been reported.[14b] For a wide range of metals, a strong affinity was found for the mono- and diaza-crown ethers containing a phenolic group. The advantage of phenol-containing LCEs might refer to the possibility of forming covalent complexes as well as complexes with ion-pair binding between the phenoxide oxygen and metal cation; moreover, the selective cation coordination by these lariats is pH-dependent. It might be expected that the replacement of a phenoxy hydrogen by a methyl group, resulting in the methoxy-substituted analog of *N*,*N*′-dibenzyldiaza-18C6 (**2**), *N*,*N*′-dimethoxydibenzyldiaza-18C6 (**1**),[20] may enhance the liphophilicity in two directions—the methyl group will provide the higher solubility in lipids, while the oxygen atom of the methoxy group will enhance the water solubility. Furthermore, the oxygen atom of the methoxy group will provide an additional acceptor for hydrogen bonding. Apart from the synthesis[20] no data dealing with the complexing ability of **1** are known so far.

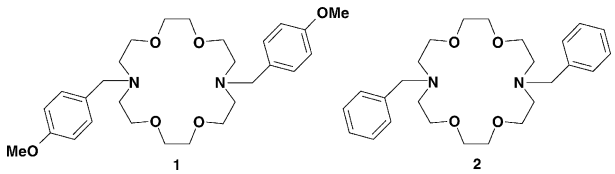

Scheme 1 Structure of lariat crown ethers.

Being involved in the host–guest chemistry based on the CEs and crowncyclophanes,[21] we, alongside others, have studied the complexation of *N*,*N*′-dibenzyldiaza-18-crown-6 (**2**) with neutral molecules.[22] In contrast to the well-developed field of metal complexation by lariat ethers only single examples of their genuine host–guest complexes are available.[23] This gap is explained by the weakness of the arising hydrogen bonding with the LCEs bearing the bulky pendant arms. This has provoked us to study the methoxy-substituted analog of **2**, *N*,*N*′-bis(4-methoxybenzyl)-1,7,10,16-tetraoxo-4,13-diazacyclooctadecane (**1**),[20] in the host–guest interactions, and compare this with the data available for **2**. For the first time the bibracchial-crown ether, 7,16-bis(4-methoxybenzyl)-1,4,10,13-tetraoxa-7,16-diazacyclooctadecane (**1**), and its molecular complex **1**·$(H_2NCS)_2$ (**3**) and proton-transfer complexes (**1**-H_2)·$[ClO_4]_2$·$2H_2O$ (**4**), (**1**-H_2)·$[NbF_6]_2$·$2H_2O$ (**5**), (**1**-H_2)·$[TaF_6]_2$·$2H_2O$ (**6**), (**1**-H_2)·$[BF_4]_2$ (**7**) and (**2**-H_2)·$[ClO_4]_2$·$2H_2O$ (**8**) were isolated and characterized by X-ray single-crystal diffraction. We intend to comparatively study the conformations of these two LCEs by computational methods in order to obtain a better insight into the conformational behavior of these kinds of compounds, and we will also try to estimate the preferable conformations for **1** and **2** depending on the degree of their protonation and the surrounding environment. We offer these results as a proof that the computational technique has now advanced to the point where calculated geometries and conformational energies of relatively complicated crown–ethers complexes are in agreement with the experimental findings (Scheme 1).

Results and discussion

X-Ray crystallography

Free macrocycle **1** crystallizes in the centrosymmetric monoclinic space group $C2/c$ with the macrocyclic molecule residing on an inversion center giving half a molecule in the asymmetric unit. Molecule **1** with the numbering scheme is shown in Fig. 1. The same numbering is used both for **1** in **3–7** and for **2** (except for the missing methoxy group) in **8**.

In **1** the oxygen atoms are arranged in an *endo*-dentate mode typical for most crowns, while the nitrogen atoms flip to an *exo*-dentate mode to incorporate binding of the methoxybenzyl

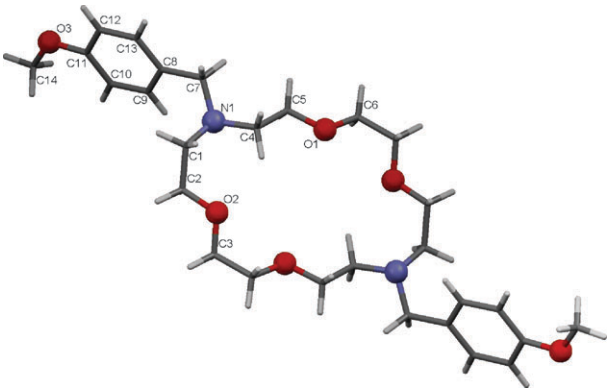

Fig. 1 Compound **1**: view with the numbering scheme.

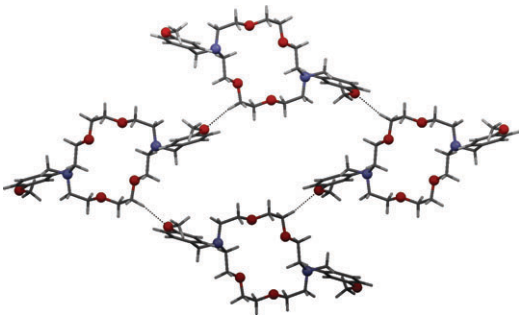

Fig. 2 Fragment of crystal packing in **1** showing the association of the molecules in a sheet *via* CH···O hydrogen bond, H···O 2.46, C···O 3.417(3) Å, CHO angle 169°.

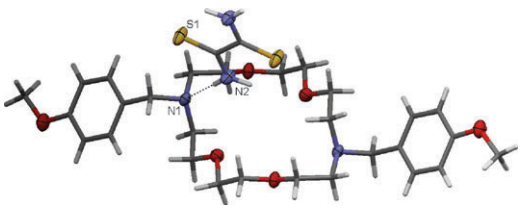

Fig. 3 View of **3** with the partial numbering scheme. Hydrogen bonding is shown by dotted lines.

groups. The molecule adopts a typical elliptical shape (Fig. 1) with two inversion-related methylene hydrogens turned inward toward the center of the ring. The two nitrogen atoms extend out in a *trans*-fashion, deviating from the plane of four oxygen atoms at ±0.884(3) Å. The conformation of the asymmetric part of the crown molecule is described by the sequence of four consecutive bonds in *trans*-conformation, followed by the *gauche*, *gauche*, *trans*, *trans*, *gauche* sequence (Table 1). The comparison with the pure phases of other bibracchial diaza-18C6 derivatives[24] as well as with the 18-membered crown ethers, 18C6, *cis*-transoid-*cis*-dicyclohexano-18C6[25] shows similarities in the shape of the macrocyclic cavity and in the pattern of the torsion angles. The methoxybenzyl side arms in **1** splay out from the crown rather than being below and above the macrocyclic plane; the dihedral angle between the planes of the N_2O_4 macrocyclic heteroatoms and the phenyl ring of the side arm is equal to 66.35(6)°.

The crystal packing for **1** clearly demonstrates the contribution of the methoxy group to the whole system of intermolecular interactions (Fig. 2). The molecules *via* weak CH···O hydrogen bonds are associated in tetramers giving rise to the H-bonded sheets. Due to the *C*2/*c* crystal symmetry these sheets interpenetrate in such a way that the methyl group of the pendant arm is arranged at 2.75 Å above (and below) the macrocyclic cavity of the nearest symmetry-related molecule of **1**. Such an arrangement is very common for the complexes of 18C6 with the CH_3 group containing guests,[26] although in our case the cavity is closed by the cross-cavity interactions and no CH (methyl)···O (crown) short contacts typical for the actual host–guest complexes were found.

Fig. 3 depicts the molecular complex **3** in a 1 : 1 ratio that crystallizes in the centrosymmetric monoclinic space group *C*2/*c*. Both **1** and dithiooxamide (**dtox**) molecules reside on inversion centers. They are held together *via* a single hydrogen bond, N2···N1 = 3.096(3) Å (Table 2). The planar **dtox** molecule is inclined at an angle of 76.46(7)° to the mean plane of six N_2O_4 heteroatoms of **1**, N2 atom deviating at 2.254(2) Å from the same plane.

Two **dtox** molecules are arranged on both sides of the centrosymmetric macrocyclic cavity. The arising host–guest interactions essentially influence the conformation of the macrocyclic molecule, which in **3** has a more flat and a more circular shape (Table 4) than in the free molecule **1**, characterized by the deviation of nitrogen atoms from the plane of four macrocyclic oxygens equal to ±0.473(3) Å and transition of two C–C bonds from *trans*-conformation to the preferable

Table 1 Torsion angles (°) along the macrocyclic framework in **1**, **3–5**, **7**

Angle	**1**	**3**	**4**	**5**	**7A**	**7B**
C(6)–O(1)–C(5)–C(4)	−179.6(2)	−173.0(2)	−171.6(3)	−179.7(4)	−173.5(1)	−171.7(1)
O(1)–C(5)–C(4)–N(1)	−161.0(2)	−67.7(2)	53.8(3)	58.4(5)	43.7(1)	45.5(1)
C(5)–C(4)–N(1)–C(1)	168.2(2)	171.8(2)	56.3(3)	59.9(4)	−172.5(1)	−169.2(1)
C(4)–N(1)–C(1)–C(2)	−81.0(2)	−55.3(3)	175.6(3)	−176.0(3)	86.6(1)	89.8(1)
N(1)–C(1)–C(2)–O(2)	76.7(2)	−53.8(3)	60.4(3)	53.6(4)	55.6(1)	58.1(1)
C(1)–C(2)–O(2)–C(3)	−179.8(2)	175.6(2)	−175.1(3)	−178.9(4)	71.5(1)	73.9(1)
C(2)–O(2)–C(3)–C(6)[a]	178.0(2)	173.2(2)	−179.3(3)	177.3(4)	163.3(1)	158.3(1)
O(2)–C(3)–C(6)[a]–O(1)[a]	−71.4(2)	73.8(3)	63.8(3)	64.0(5)	63.5(1)	61.2(1)
C(3)–C(6)[a]–O(1)[a]–C(5)[a]	−178.2(2)	172.3(2)	173.8(3)	170.5(4)	177.1(1)	−178.6(1)
C(1)–N(1)–C(7)–C(8)	−66.7(2)	−65.7(3)	164.6(3)	−163.9(3)	67.35(1)	166.9(1)
C(4)–N(1)–C(7)–C(8)	169.3(2)	60.6(3)	40.1(3)	70.2(4)	166.31(1)	−67.4(1)

[a] Symmetry transformations used to generate equivalent atoms: $a - x + 1/2, -y + 3/2, -z + 1$ (**1**); $-x + 1, -y + 1, -z$ (**3**); $-x + 1, -y + 1, -z + 1$ (**4**); $-x + 2, -y + 1, -z + 2$ (**5**); $-x + 1, -y + 1, -z$ (**7A**); $-x + 2, -y + 2, -z + 1$ (**7B**).

Table 2 Hydrogen bond distances (Å) and angles (°) in **3–5**, **7**, **8**

D–H···A	*d*(D–H)	*d*(H···A)	*d*(D···A)	∠(DHA)	Symmetry transformation for acceptor
3					
N(2)–H(2N)···N(1)	0.94(2)	2.16(3)	3.096(3)	179(2)	*x*, *y*, *z*
4					
N(1)–H(1N)···O(1W)	0.89(1)	1.92(3)	2.805(3)	169(2)	*x*, *y*, *z*
O(1W)–H(1W)···O(4)	1.00(4)	1.87(4)	2.818(6)	158(3)	*x*, *y*, *z*
O(1W)–H(1W)···O(4′)	1.00(4)	2.15(6)	2.84(5)	125(3)	*x*, *y*, *z*
O(1W)–H(2W)···O(2)	0.83(4)	2.17(5)	2.995(4)	172(4)	1 − *x*, 1 − *y*, 1 − *z*
5					
N(1)–H(1N1)···O(1W)	0.88	2.00	2.874(5)	174	*x*, *y*, *z*
O(1W)–H(2W)···O(2)	0.91	2.03	2.928(5)	170	2 − *x*, 1 − *y*, 2 − *z*
O(1W)–H(1W)···F(6)	1.04	2.12	3.043(6)	147	1 − *x*, 1 − *y*, 1 − *z*
7					
N(1A)–H(1A)···O(2A)	0.91(2)	2.35(1)	2.864(1)	116(1)	*x*, *y*, *z*
N(1B)–H(1B)···O(2B)	0.92(2)	2.40(1)	2.889(1)	114(1)	*x*, *y*, *z*
8					
N(1)–H(1N)···O(1W)	0.90(3)	1.90(3)	2.792(3)	171(3)	−*x*, −*y*, 1 − *z*
O(1W)–H(1W)···O(1)	0.73(5)	2.27(5)	2.989(3)	173(5)	*x*, *y*, *z*
O(1W)–H(2W)···O(6′)	0.89(5)	2.01(5)	2.90(1)	173(4)	*x*, *y*, *z*
O(1W)–H(2W)···O(6)	0.89(5)	2.02(5)	2.893(7)	167(4)	*x*, *y*, *z*

Table 3 Comparison of calculated structures of neutral **1** and **2** with experimental solid-state structures[a]

	1	Calculated structure **1**			Calculated structure **2**	
	Experimental structure	Vacuum	Methanol	Experimental structure, XESSUJ01	Vacuum	Methanol
N···N′	7.696	7.925	7.926	7.298	7.925	7.920
O1···O1′	4.565	4.690	4.754	4.578	4.678	4.747
O2···O2′	6.124	6.388	6.403	6.809	6.386	6.412
i-C···*i*-C′	12.518	12.727	12.729	12.207	12.715	12.719
C1–N1–CH_2–C_{ipso}	−66.65	−68.66	−70.43	−74.40	−69.21	−70.09
C4–N1–CH_2–C_{ipso}	169.31	160.01	159.42	167.84	159.06	159.46

[a] The coordinates for **2** were taken from CSD (ref. code XESSUJ01).

gauche-conformation (Table 1). In spite of these pronounced changes, the macrocycle in **3** retains its extended conformation with the twisting angle between the planes of the macrocyclic N_2O_4 heteroatoms and phenyl ring of the side arm equal to 33.78(7)°. The recently described complex **2**·$(H_2NCS)_2$[22], similarly to **3**, crystallizes as a 1 : 1 tape where the components alternate. Similar to all previously reported **dtox** complexes with CEs including complex **2**·$(H_2NCS)_2$ no short contact **dtox**···**dtox** were found in **3**. Similar to **1**, the contribution of the methoxy oxygen atom to the intermolecular CH···O interactions is essential although the H···O distance slightly exceeds the parameter typical for the conventional hydrogen bond. Due to these interactions, the tapes are packed in a zipper-like mode providing their partial interpenetration and giving rise to the layer. Following the recent investigation by Gdaniec and co-workers,[27] we can also mention here the multiple CH···S interactions, which contribute to the stability of the layer in **3** (Fig. 4).

A search of the CSD[28] and our own efforts to expand this family of complexes led us to conclude that the genuine molecular host–guest complexes are rather rare for LCEs. The most preferable guest for them is a water molecule that, due to its small size, is easily accommodated on both sides of the macrocyclic cavity.[23] In the complexes with **dtox**, 4-nitrophenylsulfonamide,[22] and malononitrile,[23a] the components are held together *via* conventional NH(CH)···$O(N)_{crown}$ hydrogen bonds.

Compounds **4–8** represent the proton-transfer complexes built up of doubly protonated macrocyclic cations, $(\mathbf{1}\text{-}H_2)^{2+}$ in **4–7** or $(\mathbf{2}\text{-}H_2)^{2+}$ in **8** and inorganic anions. The N-bound H-atoms were objectively localized in the difference Fourier maps. All except **7** represent the crystal hydrates with the water molecules incorporated between the charged species; complexes **4** and **8**, which differ by the LCE used, have a similar composition and structure and will be discussed in a sequential order, while complexes **5** and **6** are isomorphous, and so only **5** will be discussed in detail. All compounds crystallize in centrosymmetric space groups, and the macrocyclic cations $(\mathbf{1}\text{-}H_2)^{2+}$ and $(\mathbf{2}\text{-}H_2)$ exhibit a crystallographically imposed C_i symmetry. The protonation of the macrocyclic nitrogen atoms causes dramatic changes in the macrocyclic shape and in the arrangement of the pendant arms in comparison with the neutral molecules (Table 5). Complexes **4** (Fig. 5) and **8** (Fig. 6) crystallize in triclinic space group $P\bar{1}$, with similar unit cell dimensions (Table 6). The macrocyclic cations reside on an inversion center. The water molecule and the $[ClO_4]^-$ anion occupy general positions, with the latter being disordered over two sites; hence, only its major component is shown in Fig. 5 and 6. Two water molecules are located on either side of the macrocyclic cavity and reside at

Table 4 Comparison of calculated equilibrium structures of neutral **1** and **2** in **3** and **2**·$(H_2NCS)_2$[a] with experimental solid-state structures

	3	Calculated structure		**2**·$(H_2NCS)_2$ (**A**)	Calculated structure **2A**		**2**·$(H_2NCS)_2$ (**B**)	Calculated structure **2B**	
	Experimental structure	Vacuum	Methanol	Experimental structure	Vacuum	Methanol	Experimental structure	Vacuum	Methanol
N···N′	7.014	6.688	7.074	6.707	6.819	6.687	6.326	6.699	6.784
O1···O1′	4.388	5.172	4.920	5.537	5.818	5.958	5.299	5.554	5.491
O2···O2′	5.673	6.033	5.831	6.216	6.380	6.463	7.192	6.921	7.062
i-C···*i*-C′	11.879	11.178	12.013	11.370	11.575	11.487	11.343	11.803	10.671
C1–N1–CH_2–C_{ipso}	−60.61	−66.32	−64.53	−58.55	−69.67	−66.01	−62.14	−64.43	−66.21
C4–N1–CH_2–C_{ipso}	65.69	74.61	68.91	69.04	70.74	68.42	64.10	74.02	67.48

[a] In **2**·$(H_2NCS)_2$ **2** is present in two conformations, both of them were optimized.

Fig. 4 Fragment of crystal packing in **3** showing the association of molecular complexes in the layer *via* NH···N hydrogen bond and weak CH···O and CH···S interactions, H···O 2.65, C···O 3.533(3) Å, CHO angle 159°, H···S 2.93 and 2.98, C···S 3.551(3) and 3.684(3) Å, CHS angles 120° and 135°.

1.805(3) Å (**4**) and 1.678(3) Å (**8**), respectively, above the macrocyclic plane in a twin pseudo-perched orientation. In both complexes, the nitrogen atom adopts an *endo*-orientation, with their hydrogen atom being involved in NH···O hydrogen bonding with the lone pair of the water molecule. In turn, the water molecule, acting as a H-donor, provides both of its hydrogens for the OH···O interactions with one oxygen atom of the crown molecule and one oxygen atom of the $[ClO_4]^-$ anion (Table 2). Thus, the water molecule exhibits its traditional mediating function between the charged species.[29] A very similar example gives *N*,*N*′-dibenzyl-4,13-diazonia-18-crown-6 tetrachloro-dioxo-uranium dihydrate (**2**-H_2)(UCl_4O_2)·$2H_2O$,[8] where two water molecules bind to the inner cavity of the crown ether in a symmetry-related mode. For both protonated macrocycles, we observe the further tendency toward more circular (Tables 4 and 5) and more planar shapes in comparison with the neutral molecules; the deviation of the nitrogen atoms from the plane through the macrocyclic oxygens is equal to ±0.606(4) Å and ±0.629(3) Å in $(\mathbf{1}\text{-}H_2)^{2+}$ and $(\mathbf{2}\text{-}H_2)^{2+}$, respectively. The twisting angle between the N_2O_4 and C8–···–C13 planes is equal to 62.76(9) in **4** and 77.45(8) in **8**, respectively.

The distinction in the twisting angle values is most probably dictated by the involvement of the methoxy group in the intermolecular interactions with the inversion-related macrocyclic cations with the formation of $R_2^2(\mathbf{8})$ planar supramolecular synthon (Fig. 7a), while in **8** the aryl substituents are displayed in parallel planes with an interplane distance of 3.330 Å (Fig. 7b).

Recently,[30a] we have succeeded in using aza-CEs, namely aza-15C5 and aza-18C6, under synthetic conditions identical to those described in the Experimental part of this article to elicit the rather unusual anionic forms for Nb and Ta, $[(H_2O)NbF_4ONbF_5]^-$ and $[(TaF_5)_2O]^{2-}$, respectively. However, the use of **1** yielded two isomorphous complexes **5** and **6** (Table 3), with the $[NbF_6]^-$ and $[TaF_6]^-$ hexafluorometallate anions as the counter-ions being typical for the oxonium complexes of O-containing CEs.[30b] In **5** and **6** both $[NbF_6]^-$ and $[TaF_6]^-$ have an octahedral geometry, with the Nb–F and Ta–F distances being in the range 1.852(4)–1.879(2) and 1.856(8)–1.885(8) Å, respectively. In **5** the $(\mathbf{1}\text{-}H_2)^{2+}$ cation and the two crystallographically unique $[NbF_6]^-$ anions reside on inversion centers, while the water molecule occupies the general position (Fig. 8). Similar to **4** and **8**, the water molecule

Table 5 Comparison of calculated equilibrium structures of doubly protonated macrocycles $(\mathbf{1}\text{-}H_2)^{2+}$ and $(\mathbf{2}\text{-}H_2)^{2+}$ in **4–8** with experimental solid-state structures

	4			**8**			**5**		
	Experimental structure	Vacuum	Methanol	Experimental structure	Vacuum	Methanol	Experimental structure	Vacuum	Methanol
N···N′	6.357	6.623	6.394	6.242	6.630	6.529	6.432	6.626	
O1···O1′	4.443	4.907	4.770	4.797	4.868	4.857	4.697	4.858	
O2···O2′	5.789	5.328	5.515	5.744	5.361	5.425	5.547	5.418	
i-C···*i*-C′	10.405	9.498	8.972	9.722	9.677	9.114	9.550	9.911	
C1–N1–CH_2–C_{ipso}	−40.10	−59.98	−66.09	−62.67	−58.00	−65.46	−70.22	−53.85	
C4–N1–CH_2–C_{ipso}	164.61	174.01	168.03	174.09	176.05	169.20	163.83	179.79	

	7(A)			**7(B)**			$(\mathbf{2}\text{–}H_2)[BF_4]_2\cdot H_2O$		
	Experimental structure	Vacuum	Methanol	Experimental structure	Vacuum	Methanol	Experimental structure	Vacuum	Methanol
N···N′	5.641	6.351	6.197	5.684	6.363	6.138	5.841	6.306	6.121
O1···O1′	5.088	4.558	4.564	4.792	4.533	4.604	4.469	4.471	4.633
O2···O2′	5.106	5.265	5.323	5.324	5.262	5.321	5.449	5.301	5.341
i-C···*i*-C′	6.619	8.438	7.714	6.660	8.376	7.626	6.995	7.932	7.658
C1–N1–CH_2–C_{ipso}	−67.35	−60.79	−68.90	−67.40	−62.23	−67.40	−69.62	−66.32	−65.86

Fig. 5 View of **4** with the partial numbering scheme. Only the major position for the disordered anion is shown. Hydrogen bonding is shown by dotted lines. The atom with the suffix A is at the symmetry position $(1 - x, 1 - y, 1 - z)$.

Fig. 6 View of **8** with the partial numbering scheme. Only the major position for the disordered anion is shown. Hydrogen bonding is shown by dotted lines. Atoms with the suffix A are at the symmetry position $(-x, -y, 1 - z)$.

mediates charged species as a single acceptor with the crown's NH^+ group *via* an $NH^+\cdots O$ (water) hydrogen bond and as a double donor *via* OH (water)···O and OH (water)···F hydrogen bonds with one oxygen atom of the macrocycle and one fluorine atom of the anion (Table 2). It is located at 1.577(5) Å (1.678(3) Å in **6**) above the mean plane of the N_2O_4 set of heteroatoms. Only one anion, $[Nb(2)F_6]^-$, makes contact with the intermediate water molecule, while the other, $[Nb(1)F_6]^-$, is involved in the CH···F intermolecular interactions, thus being interspersed between a network of crown molecules (Fig. 9). The *trans-annular* N···N and O···O distances across the cavity and the sequence of torsion angles along the macrocyclic framework in the $(\mathbf{1}\text{-}H_2)^{2+}$ cation are very close to those of **4**, while the orientation of the side arms differs as indicated by the twisting angle of 75.03(9)° between the planes through the N_2O_4 set and the phenyl ring.

The explanation for the different turn of the pendant arms in **4** and **5** may follow from slightly different interactions between the pendant arms of neighboring complexes, since the lone pair of the methoxy-group oxygen atom in **5(6)** is not involved in the H-bonding self-assembling interactions, and the pendant arms of inversion-related macrocycles are

Table 6 Crystal data and structure refinement parameters for **1**, **3–8**

	1	**3**	**4**	**5**	**6**	**7**	**8**
Formula	$C_{28}H_{42}N_2O_6$	$C_{28}H_{42}N_2O_6 \cdot C_2H_4N_2S_2$	$C_{28}H_{44}N_2O_6 \cdot [ClO_4]_2 \cdot 2H_2O$	$C_{28}H_{44}N_2O_6 \cdot [NbF_6]_2 \cdot 2H_2O$	$C_{28}H_{44}N_2O_6 \cdot [TaF_6]_2 \cdot 2H_2O$	$C_{28}H_{44}N_2O_6 \cdot [BF_4]_2$	$C_{26}H_{40}N_2O_4 \cdot [ClO_4]_2 \cdot 2H_2O$
Formula weight	502.64	622.83	739.58	954.50	1130.58	678.27	679.53
Crystal system	Monoclinic	Monoclinic	Triclinic	Triclinic	Triclinic	Triclinic	Triclinic
Space group	$C2/c$	$C2/c$	$P\bar{1}$	$P\bar{1}$	$P\bar{1}$	$P\bar{1}$	$P\bar{1}$
a/Å	21.436(4)	17.2050(5)	7.322(1)	6.8821(3)	6.8062(11)	11.933(2)	7.592(2)
b/Å	11.050(2)	8.4590(3)	10.757(2)	11.3041(5)	11.3381(18)	12.120(2)	10.458(2)
c/Å	12.701(3)	23.3120(9)	12.450(2)	14.0931(5)	14.098(2)	12.404(2)	10.976(2)
α/°	90.0	90.0	91.67(2)	106.232(2)	105.873(9)	94.820(1)	98.11(3)
β/°	108.86(3)	104.260(12)	104.92(3)	101.770(2)	101.336(9)	111.714(1)	94.67(2)
γ/°	90.0	90.0	109.41(3)	106.118(2)	106.175(6)	100.392(1)	108.51(3)
V/Å^3	2846.9(10)	3288.2(2)	886.6(2)	963.03(7)	960.2(3)	1616.86(5)	810.7(3)
Z	4	4	1	1	1	2	1
ρ_{calc}/g cm^{-3}	1.173	1.258	1.385	1.646	1.955	1.393	1.392
μ/mm^{-1}	0.082	0.208	0.256	0.699	5.797	0.125	0.268
F(000)	1088	1336	392	484	548	712	
Reflections collected/ unique	10373/2525	8339/2905	9404/3296	6316/3763	5444/3640	11815/6275	3162/3162
Reflections with $I > 2\sigma(I)$(R_{int})	1661 [R_{int} = 0.042]	1947 [R_{int} = 0.0655]	2039 [R_{int} = 0.041]	2854 [R_{int} = 0.0212]	2021 [R_{int} = 0.0371]	5547 [R_{int} = 0.0139]	2361 [R_{int} = 0.031]
Goodness-of-fit	1.055	0.953	1.106	1.068	0.924	1.046	1.030
R_1, wR_2 [$I > 2\sigma(I)$]	0.0456, 0.1210	0.0568, 0.1474	0.0574, 0.1599	0.0550, 0.1658	0.0546, 0.1571	0.0338, 0.0914	0.0585, 0.1668
R_1, wR_2 (all data)	0.0784, 0.1331	0.0838, 0.1595	0.1009, 0.1747	0.0688, 0.1788	0.0971, 0.1870	0.0387, 0.0943	0.0793, 0.1781

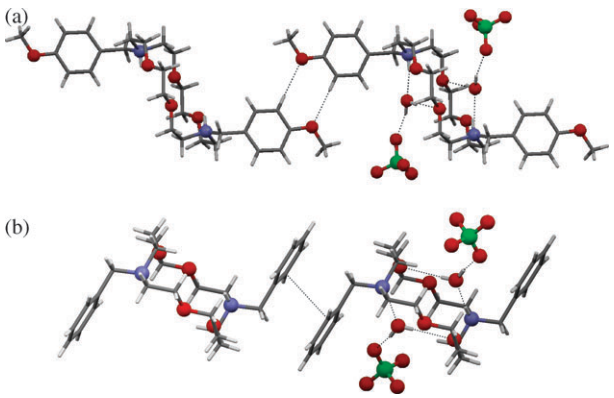

Fig. 7 (a) Self-assembling of adjacent macrocycles in **4** *via* C–H···O hydrogen bonds, H···O 2.56, C···O 3.491(4) Å, CHO angle 179°. (b) An arrangement of adjacent macrocycles in **8** with the interplane distance of 3.330 Å. The shortest intermolecular contacts are shown by dotted lines.

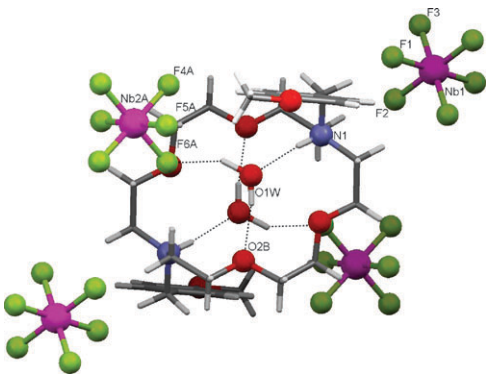

Fig. 8 View of **5** with the partial numbering scheme. Hydrogen bonding is shown by dotted lines. Atoms with the suffixes A and B are at the symmetry positions (1 − x, 1 − y, 1 − z) and (2 − x, 1 − y, 2 − z), respectively.

arranged in parallel planes with a partial overlap typical for the π–π interactions (Fig. 9).

Compound **7** of the 1 : 2 ratio crystallizes in the triclinic space group $P\bar{1}$. The asymmetric unit contains two halves of two macrocyclic cations (labeled **A** and **B**) that reside on two different inversion centers and two $[BF_4]^-$ anions (also labeled **A** and **B**) in general positions. The conformations of the two macrocycles (Tables 1 and 5) and the geometry of the two $[BF_4]^-$ anions are very similar, and so only the components labeled **A** are shown in Fig. 10.

Of the proton-transfer complexes discussed herein, only **7** represents a water-free compound. The protonated macrocyclic nitrogen atoms adopt an *endo*-orientation that is stabilized by the short-cut intramolecular N–H···O distance (Table 2). The macrocyclic cavity adopts a chair conformation with the deviation of nitrogen atoms at ±1.507(1) Å (±1.511(1) Å in

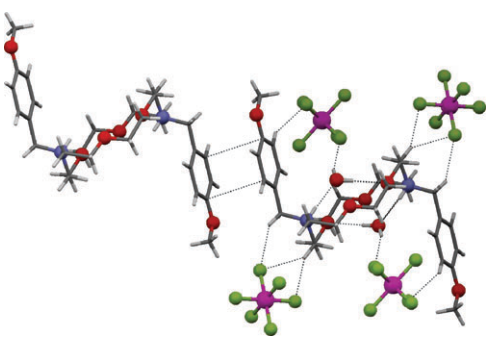

Fig. 9 Fragment of crystal packing in **5** showing the association of the adjacent macrocycles. The interplane separation between the aromatic units is equal to 3.389 Å. The shortest CH···F intermolecular contacts H···F 2.52–2.64, C···F 3.308(3)–3.461(3) Å, CHF angle 136°–154° are shown by dotted lines.

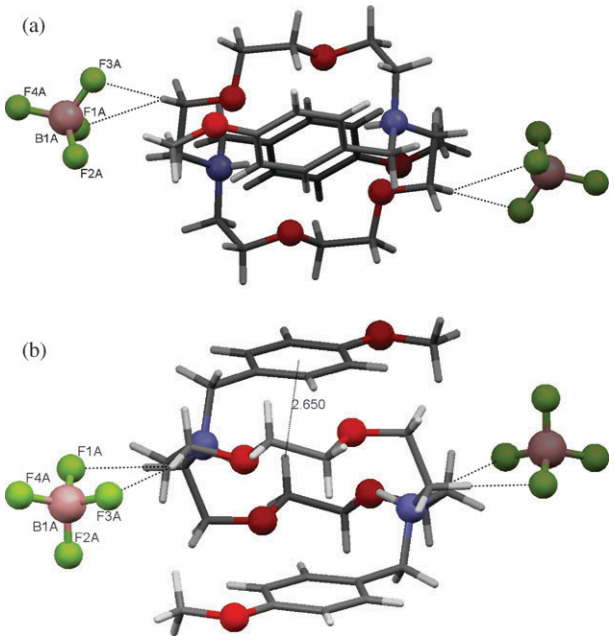

Fig. 10 Top (a) and side (b) views of complex **7A** with the partial numbering scheme. The shortest CH···F intermolecular contacts H···F 2.54 and 2.59, C···F 3.485(4) and 3.130(4) Å, CHF angle 164° and 115° are shown by dotted lines. (b) C–H···π interaction is shown by a dotted line.

cation **B**) from the plane of four oxygen atoms, the value being maximal among all the complexes described here. The C–H···π interactions between two methylene hydrogens and aromatic subunits effectively turn the phenyl groups of the side arms above and below the macrocycle (Fig. 10b) in such a way that the dihedral angle between the plane of the aromatic ring and the plane of the crown oxygen atoms is 43.17(4)° (45.46(4)° for cation **B**). Both of these types of intramolecular interactions were previously noted in the parent $(\mathbf{2}\text{-}H_2)^{2+}$ in the series of lanthanoid complexes,[8] in $(\mathbf{2}\text{-}H_2)I_8$,[12] and in $(\mathbf{2}\text{-}H_2)[BF_4]_2\cdot H_2O$.[11] Inspection of torsion angles (Table 1) reveals that the macrocycle is characterized by the energetically preferable *gauche*- and *trans*-conformations along the C–C and C–O bonds, while N–C bonds are equally distributed between *gauche*- and *trans*-conformations. The pendant arms of the symmetry-related macrocycles demonstrate the same type of self-association as in **5** (Fig. 11).

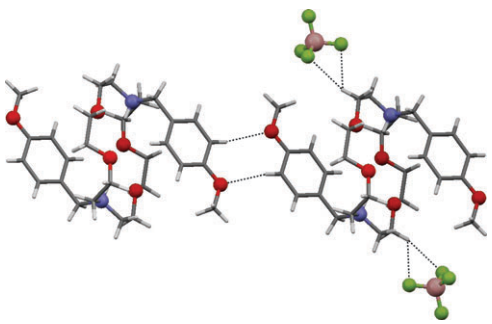

Fig. 11 Fragment of crystal packing in **7**. Self-assembling of adjacent macrocycles (labeled **A**) *via* C–H···O hydrogen bond, H···O 2.57, C···O 3.452(4) Å, CHO angle 160°. The shortest intermolecular contacts are shown by dotted lines.

The reported data represent three types of complexes: the genuine host–guest complex **3** with the conventional hydrogen bonds as the main interactions between the components, the proton-transfer ternary complexes **4–6**, **8** with the water molecule incorporated between the charged species, and the binary water-free complex **7**. Our own results and recent literature data providing the structural information make it possible to compare the conformations of **1** and **2** with the related structure complexes and to estimate the influence of minor changes in the macrocycle (the methoxy group incorporated into the pendant arm) on the conformation of the macrocycle and the overall system of interactions.

Quantum chemical calculations

Herein we have completed the X-ray data by quantum chemical calculations on the DFT level of theory that provide in-depth details on the conformations of **1** and **2** macrocycles, and especially on the positions of the pendant arms. Calculations were performed in the gas phase and in methanol to simulate the solvation effects. Since the relevant experimental structures exhibited crystallographically imposed inversion symmetry, all quantum chemical calculations were also performed with that symmetry restriction. For all structures, the optimization of the geometry of the macrocycle in vacuum and in methanol solution has been carried out and the results are summarized in Tables 3–5. All the calculated conformers are very close to the parent X-ray structures. In general, for all optimized structures, the shape of the macrocycle (measured by the distances of opposite facing heteroatoms) and the position of the pendant arms measured by the distance of two *ipso*-C atoms (atom C7 and its symmetry-related counterpart in Fig. 1) are close to the experimental solid-state structures (see Tables 3–5). The comparison of two sets of optimization carried out in vacuum and in methanol reveals the best fit of crystalline data with the vacuum structure for free **1**, while for the complexed macrocycle the best fit was obtained when the solvation effects were taken into consideration, *i.e.* for the optimization made in methanol. Fig. 12 summarizes the equilibrium structures for **1** and $(\mathbf{1}\text{-}H_2)^{2+}$ in **1**, **3–7**.

Ab initio HF/6-31+G quantum chemical calculations have been performed for the complexation energy for pairs of compounds $\mathbf{1}\cdot(H_2NCS)_2$, (**3**) and $\mathbf{2}\cdot(H_2NCS)_2$, and

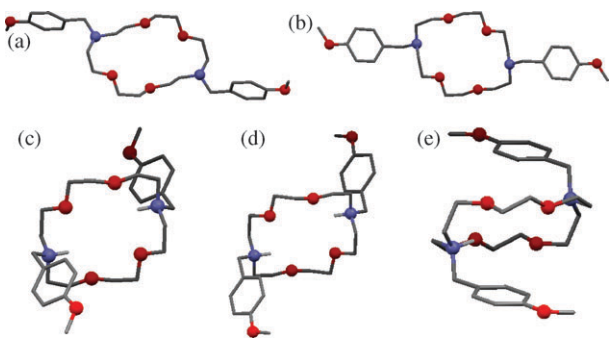

Fig. 12 Calculated equilibrium structures for neutral **1** and $(\mathbf{1}\text{-}H_2)^{2+}$ cation from **1**, **3–7**. All C-bound H-atoms are omitted for clarity. (a) free **1** (vacuum); (b) neutral **1** from **3** (methanol); (c) $(\mathbf{1}\text{-}H_2)^{2+}$ from **4** (methanol); (d) $(\mathbf{1}\text{-}H_2)^{2+}$ from **5** (vacuum); (e) $(L^1H_2)^{2+}$ from **7** (methanol).

(**1**-H_2)·$[BF_4]_2$ (**7**) and (**2**-H_2)·$[BF_4]_2$·H_2O, where the water molecules are not incorporated between the host and guest molecules. The complexation energy was estimated as $\Delta E = E_{Complex} - E_{Host} - E_{Guest}$. The complexation energies of −724.844 kcal mol^{-1} for complex **7** and −762.558 kcal mol^{-1} for (**2**-H_2)·$[BF_4]_2$·H_2O show a better complexation efficiency for the proton-transfer complexes than for the molecular complexes, −16.996 kcal mol^{-1} for **1**·$(H_2NCS)_2$, (**3**), and −12.408 kcal mol^{-1} for **2**·$(H_2NCS)_2$.

Conclusion

We have reported the synthesis, and X-ray and DFT studies for the molecular and proton-transfer complexes based on unexplored bibracchial-crown ether, *N*,*N*′-dimethoxydibenzyl-1,7,10,16-tetraoxo-4,13-diazacyclooctadecane (**1**). The available data demonstrate the pronounced conformational mobility of macrocyclic cavity and distinctions in the orientation of pendant arms. Moreover, the nature of the anion strongly influences the twisting of the pendant group, making it orient in opposite directions. To rationalize different conformations of **1** in comparison with the parent *N*,*N*′-bis(4-methoxybenzyl)-1,7,10,16-tetraoxo-4,13-diazacyclooctadecane (**2**), theoretical quantum chemical calculations on the DFT (B3LYP) level were performed. All calculated conformers are close to the initial X-ray structures. The investigation shows that the computational approach correlates with the structural findings. We can conclude that we can emulate in the calculations the weak force interactions that we observe in the solid-state structures. The methoxy group that contributes by the C–H···O(OCH_3) hydrogen bonding to the overall system of intermolecular interactions imposes distinctions both in the orientation of pendant arms in particular and in the crystal packing as a whole.

Experimental

General

Caution! Although we have experienced no difficulties with the perchloric and hydrofluoric acids, these should be regarded as potentially dangerous substances and handled with care. Commercially available reagents were used as received. Compounds **3–8** were analyzed for C, H, and N in a Perkin Elmer 240C. The thin layer chromatographic control of the purity of substances was performed on Silufol UV-254 plates. All compounds were synthesized by an addition of the corresponding 'guest' species directly to a stirred solution of the LCE. Moderate heating was required to complete full dissolution. The composition of all compounds was confirmed by routine elemental analysis.

(1). The initial ligand was synthesized following the procedure described earlier.[20]

1·$(H_2NCS)_2$ (3). **1** (125 mg, 0.25 mmol) and ethanedithioamide (30 mg, 0.25 mmol) were dissolved in methanol (3 ml) at 64 °C, followed by the addition of ethyl acetate (3 ml) and *n*-butanol (1 ml). The resulting clear solution was slowly reduced in volume by evaporating the solvents at room temperature. Red transparent crystals were obtained, mp 108–110 °C. Analysis: found: C, 57.81, H, 7.49, N, 9.06, S, 10.33%; $C_{30}H_{46}N_4O_6S_2$: calc.: C, 57.85, H, 7.44, N, 9.00, S, 10.30%.

(1-H_2)·$[ClO_4]_2$·$2H_2O$ (4). To **1** (50 mg, 0.1 mmol) dissolved in methanol (5 ml) was added 70% perchloric acid (0.7 ml) dissolved in methanol (2 ml) at 64 °C, followed by the addition of ethyl acetate (4 ml). The resulting clear solution was slowly reduced in volume by evaporating the solvents at room temperature. Colorless transparent crystals were obtained, mp 132–134 °C. $C_{28}H_{48}Cl_2N_2O_{16}$: calc.: C, 45.47; H, 6.54; N, 3.79%. Found: C, 45.43; H, 6.57; N, 3.82%.

(1-H_2)·$[NbF_6]_2$·$2H_2O$ (5). To niobium oxide (v) (133 mg, 0.5 mmol) was added 45% hydrofluoric acid (10 ml). The resulting solution was boiled till the volume of 4–5 ml was reached. To the obtained acidic solution was added a solution of **1** (251 mg, 0.5 mmol) in methanol (10 ml). The resulting crystals were removed from the solution before the solvent had completely evaporated. Colorless transparent crystals of the complex were obtained, mp 185–187 °C (dec.). The yield is almost quantitative. $C_{28}H_{48}F_{12}N_2Nb_2O_8$: calc.: C, 35.23; H, 5.07%; F, 23.89; N, 2.93%. Found: C, 35.28; H, 5.02; F, 23.86; N, 2.96%.

(1-H_2)·$[TaF_6]_2$·$2H_2O$ (6). To tantalum oxide (v) (221 mg, 0.5 mmol) was added 45% hydrofluoric acid (10 ml). The resulting solution was boiled till the volume of 4–5 ml was reached. To the obtained acidic solution was added a solution of L^1 (251 mg, 0.5 mmol) in methanol (10 ml). The resulting crystals were removed from the solution before the solvent had completely evaporated. Colorless transparent crystals of the complex were obtained, mp 185–187 °C (dec.). The yield was almost quantitative. $C_{28}H_{48}F_{12}N_2O_8Ta_2$: calc.: C, 29.75; H, 4.28; F, 20.17; N, 2.48%. Found: C, 29.71; H, 4.25; F, 20.21; N, 2.44%.

(1-H_2)·$[BF_4]_2$ (7). To L^1 (50 mg, 0.1 mmol) dissolved in methanol (5 ml) boron trifluoride etherate (0.35 ml) was added. The resulting clear solution was slowly reduced in volume by evaporating the solvents at room temperature. Colorless transparent crystals were obtained by recrystallization from a methanol–ethyl acetate mixture (1 : 2), mp 132–134 °C. $C_{28}H_{44}B_2F_8N_2O_6$: calc.: C, 49.58; H, 6.54; F, 22.41; N, 4.13%. Found: C, 49.54; H, 6.59; F, 22.47; N, 4.15%.

(2-H_2)·$[ClO_4]_2$·$2H_2O$ (8). To **2** (44 mg, 0.1 mmol) dissolved in a mixture of methanol (5 ml) and *n*-BuOH (0.5 ml) was added 70% perchloric acid (0.3 ml). The resulting clear solution was slowly reduced in volume by evaporating the solvents at room temperature. Colorless transparent crystals were obtained, mp 154–155 °C. $C_{26}H_{44}Cl_2N_2O_{14}$: calc.: C, 45.95; H, 6.53; N, 4.12%. Found: C, 45.92; H, 6.57; N, 4.10%.

X-Ray crystallographic data for 1, 3–8. The X-ray data and the details of the refinement for **1**, **3–8** are given in Table 6; the torsion angles and H-bonding data are summarized in Tables 1 and 2, respectively. Tables 3–5 contain the geometric parameters for **1**, **2** and their protonated forms for the experimental solid-state and calculated structures. The X-ray intensity data for **1**, **3–5** and **8** were collected at

room temperature on a Nonius Kappa CCD diffractometer[31] while for **6** and **7** they were collected on a Bruker CCD diffractometer—both diffractometers were equipped with graphite monochromated Mo-Kα radiation. Unit cell parameters were obtained and refined using the whole data set. Frames were integrated and corrected for Lorentz and polarization effects using DENZO.[32] The scaling and the global refinement of the crystal parameters were performed by SCALEPACK.[32] For **5** and **6**, the absorption correction using SADABS was applied.[33] The structure solution and refinement proceeded similarly for all structures using the SHELX-97 program package.[34] Direct methods yielded all non-hydrogen atoms of the asymmetric unit. These atoms were treated anisotropically (full-matrix least squares method on F^2). In **4** the oxygen atoms of the $[ClO_4]^-$ anion are disordered over two positions with occupancies of 0.86(1) and 0.14(1), respectively, and only the major component was treated anisotropically. In **7** the oxygen atom of the water molecule was refined with the partial occupancy of 0.17(2) in an isotropic approximation. Hydrogen atoms in the water molecule were not localized. In **8** three oxygen atoms O4, O5, and O6 of the $[ClO_4]^-$ anion are disordered over two positions with occupancies of 0.75(1) and 0.25(1), respectively; the major component was treated anisotropically and the minor position was treated in an isotropic approximation. In all structures, C-bound H atoms were placed in the calculated positions and were treated using a riding-model approximation, with $U_{iso}(H) = 1.2\ U_{eq}(C)$ for methylene and $U_{iso}(H) = 1.5\ U_{eq}(C)$ for methyl groups, respectively, while the N- and O-bound H-atoms were found from differential Fourier maps at an intermediate stage of the refinement and were treated isotropically. All images were produced using Mercury.[35]

Computational details. *Ab initio* calculations were carried out using density functional theory with the Gaussian03 package at the B3LYP/6-31+G and HF/6-31+G levels of theory.[36] To avoid SCF convergence problems, a quadratic convergence procedure was applied during the geometry optimizations. Full geometry optimizations of the studied compounds were performed both in solution and in the gas phase. The polarizable continuum model (PCM) was included in the SCF procedure for the description of the methanol solutions with the exception of **4**. The dielectric constant was set at 32.63. All calculations were carried out using the restricted spin formalism (closed-shell).

Acknowledgements

The diffraction data for **1**, **4** and **8** were collected at the Schulich Faculty of Chemistry, Technion, Haifa, through the cooperation of Prof. Menahem Kaftory, whom we would like to acknowledge. The authors thank Prof. A. S. Dimoglo for the computational facility.

References

1 C. J. Pedersen, *J. Am. Chem. Soc.*, 1967, **89**, 7017.
2 C. J. Pedersen, *J. Am. Chem. Soc.*, 1967, **89**, 2495.
3 M. E. Weber, E. K. Elliott and G. W. Gokel, *Org. Biomol. Chem.*, 2006, **4**, 83.
4 V. J. Gatto and G. W. Gokel, *J. Am. Chem. Soc.*, 1984, **106**, 8240.
5 K. A. Arnold, A. M. Viscariello, M. Kim, R. D. Gandour, F. R. Fronczek and G. W. Gokel, *Tetrahedron Lett.*, 1988, **29**, 3025.
6 (*a*) G. W. Gokel, W. M. Leevy and M. E. Weber, *Chem. Rev.*, 2004, **104**, 2723; (*b*) G. W. Gokel, *Chem. Soc. Rev.*, 1992, **21**, 39.
7 K. R. Fewings and P. C. Junk, *Aust. J. Chem.*, 1999, **52**, 1109.
8 D. J. Evans, P. C. Junk and M. K. Smith, *New J. Chem.*, 2002, **26**, 1043.
9 M. I. Saleh, A. Salhin, B. Saad and H.-K. Fun, *J. Mol. Struct.*, 1999, **475**, 93.
10 T. W. Hambley, L. F. Lindoy, J. R. Reimers, P. Turner, G. Wei and A. N. Widmer-Cooper, *J. Chem. Soc., Dalton Trans.*, 2001, 614.
11 S. S. Basok, L. Croitoru, M. S. Fonari, E. V. Ganin, V. O. Gelmboldt, J. Lipkowski and Yu. A. Simonov, *Acta Crystallogr., Sect. C: Cryst. Struct. Commun.*, 2005, **61**, o188.
12 A. S. Gaballa, S. M. Teleb, E. Rusanov and D. Steinborn, *Inorg. Chim. Acta*, 2005, **357**, 4144.
13 P. C. Junk and M. K. Smith, *Inorg. Chem. Commun.*, 2002, **5**, 1082.
14 (*a*) E. K. Elliott, J. Hu and G. W. Gokel, *Supramol. Chem.*, 2007, **19**, 175; (*b*) A. V. Bordunov, J. S. Bradshaw, X. X. Zhang, N. K. Dalley, X. Kou and R. M. Izatt, *Inorg. Chem.*, 1996, **35**, 7229; (*c*) A. Awasthy, M. Bhatnagar, J. Tomar and U. Sharma, *Bioinorg. Chem. Appl.*, 2006, **2006**, 1.
15 (*a*) J. Hu, L. J. Barbour, R. Ferdani and G. W. Gokel, *Chem. Commun.*, 2002, 1806; (*b*) J. Hu, L. J. Barbour and G. W. Gokel, *Chem. Commun.*, 2002, 1808; (*c*) J. Hu, L. J. Barbour, R. Ferdani and G. W. Gokel, *Chem. Commun.*, 2002, 1810.
16 L. G. A. van de Water, W. Buijs, W. L. Driessen and J. Reedijk, *New J. Chem.*, 2001, **25**, 243.
17 M. Grotjahn and E. Kleinpeter, *J. Mol. Model*, 1999, **5**, 296.
18 (*a*) C.-C. Su and L.-H. Lu, *J. Mol. Struct.*, 2004, **702**, 23; (*b*) C.-C. Su, L.-H. Lu and T.-J. Hsieh, *J. Mol. Struct.*, 2007, **831**, 151.
19 (*a*) C. Platas-Iglesias, D. Esteban-Gómez, T. Enríquez-Pérez, F. Avecilla, A. de Blas and T. Rodríguez-Blas, *Inorg. Chem.*, 2005, **44**, 2224; (*b*) C. Platas-Iglesias, D. Esteban, V. Ojea, F. Avecilla, A. de Blas and T. Rodríguez-Blas, *Inorg. Chem.*, 2003, **42**, 4299; (*c*) M. González-Lorenzo, C. Platas-Iglesias, F. Avecilla, S. Faulkner, S. J. A. Pope, A. de Blas and T. Rodríguez-Blas, *Inorg. Chem.*, 2005, **44**, 4254.
20 N. G. Lukyanenko, S. S. Basok, E. Yu. Kulygina and V. I. Vetrogon, *Russ. J. Gen. Chem.*, 2003, **73**, 1919.
21 (*a*) M. S. Fonari, Yu. A. Simonov, Yu. M. Chumakov, G. Bocelli, E. V. Ganin and A. A. Yavolovskii, *Supramol. Chem.*, 2004, **16**, 23; (*b*) N. G. Lukyanenko, T. I. Kirichenko, A. Yu. Lyapunov, C. Yu. Kulygina, Yu. A. Simonov, M. S. Fonari and M. M. Botoshansky, *Tetrahedron Lett.*, 2004, **45**, 2927; (*c*) M. S. Fonari, Yu. A. Simonov, G. Bocelli, M. M. Botoshansky and E. V. Ganin, *J. Mol. Struct.*, 2005, **738**, 85; (*d*) Yu. A. Simonov, M. S. Fonari, Gh. Duca, M. V. Gonta, E. V. Ganin, A. A. Yavolovskii, M. Gdaniec and J. Lipkowski, *Tetrahedron*, 2005, **61**, 6596; (*e*) N. G. Lukyanenko, T. I. Kirichenko, A. Yu. Lyapunov, A. V. Mazepa, Yu. A. Simonov, M. S. Fonari and M. M. Botoshansky, *Chem.–Eur. J.*, 2005, **11**, 262; (*f*) E. V. Ganin, M. S. Fonari, Yu. A. Simonov, G. Bocelli, S. S. Basok, V. V. Tkachuk, S. A. Kotlyar and G. L. Kamalov, *J. Inclusion Phenom. Macrocyclic Chem.*, 2005, **52**, 63; (*g*) W.-J. Wang, E. V. Ganin, M. S. Fonari, Yu. A. Simonov and G. Bocelli, *Org. Biomol. Chem.*, 2005, **3**, 3054; (*h*) M. S. Fonari, E. V. Ganin, S.-W. Tang, W.-J. Wang and Yu. A. Simonov, *J. Mol. Struct.*, 2007, **826**, 89; (*i*) B. Moulton, B. S. Luisi, M. S. Fonari, S. S. Basok, E. V. Ganin and V. Ch. Kravtsov, *New J. Chem.*, 2007, **31**, 561.
22 M. S. Fonari, Yu. A. Simonov, L. Croitoru, S. S. Basok, E. V. Ganin and J. Lipkowski, *J. Mol. Struct.*, 2006, **794**, 110.
23 For lariat ethers host–guest molecular complexes see: (*a*) K. von Deuten, A. Knochel, J. Kopf, J. Oehler and G. Rudolph, *J. Chem. Res.*, 1979, **358**, 4035; (*b*) Y. Habata and S. Akabori, *J. Chem. Soc., Dalton Trans.*, 1996, 3871; (*c*) R. E. Gawley, S. Pinet, C. M. Cardona, P. K. Datta, T. Ren, W. C. Guida, J. Nydick and R. M. Leblanc, *J. Am. Chem. Soc.*, 2002, **124**, 13448; (*d*) Y. Habata, T. Saeki and S. Akabori, *J. Heterocycl. Chem.*, 2001, **38**, 585; (*e*) K. A. Arnold, A. M. Viscariello, M. Kim,

R. D. Gandour, F. R. Fronczek and G. W. Gokel, *Tetrahedron Lett*., 1988, **29**, 3025.

24 (*a*) S. L. De Wall, E. S. Meadows, L. J. Barbour and G. W. Gokel, *J. Am. Chem. Soc*., 1999, **121**, 5613; (*b*) L. Kh. Minacheva, I. S. Ivanova, E. N. Pyatova, V. S. Sergienko, A. Yu. Tsivadze, G. A. Artamkina and I. P. Beletskaya, *Russ. Proc. Natl. Acad. Sci. USSR*, 2003, **389**, 58; (*c*) L. Kh. Minacheva, I. S. Ivanova, E. N. Pyatova, V. S. Sergienko, G. A. Artamkina, I. P. Beletskaya and A. Yu. Tsivadze, *Crystallogr. Rep*., 2004, **49**, 982; (*d*) K. Kubo, R. Ishige, N. Kato, E. Yamamoto and T. Sakurai, *Heterocycles*, 1997, **45**, 2365; (*e*) E. S. Meadows, S. L. De Wall, L. J. Barbour and G. W. Gokel, *J. Am. Chem. Soc*., 2001, **123**, 3092; (*f*) E. S. Meadows, S. L. De Wall, L. J. Barbour, F. R. Fronczek, M.-S. Kim and G. W. Gokel, *J. Am. Chem. Soc*., 2000, **122**, 3325; (*g*) S. Suarez, O. Mamula, R. Scopelliti, B. Donnio, D. Guillon, E. Terazzi, C. Piguet and J.-C. G. Bunzli, *New J. Chem*., 2005, **29**, 1323; (*h*) G. Ulrich, P. Turek, R. Ziessel, A. De Cian and J. Fischer, *Chem. Commun*., 1996, 2461; (*i*) D. Esteban, F. Avecilla, C. Platas-Iglesias, J. Mahia, A. de Blas and T. Rodriguez-Blas, *Inorg. Chem*., 2002, **41**, 4337; (*j*) T. Gunnlaugsson, H. Q. N. Gunaratne, M. Nieuwenhuyzen and J. P. Leonard, *J. Chem. Soc., Perkin Trans. 1*, 2002, 1954; (*k*) G. McSkimming, J. H. R. Tucker, H. Bouas-Laurent, J.-P. Desvergne, S. J. Coles, M. B. Hursthouse and M. E. Light, *Chem.–Eur. J*., 2002, **8**, 3331.

25 (*a*) E. Maverick, P. Seiler, W. B. Schweizer and J. D. Dunitz, *Acta Crystallogr., Sect. B: Struct. Crystallogr. Cryst. Chem*., 1980, **36**, 615; (*b*) V. Ch. Kravtsov, M. S. Fonari, M. J. Zaworotko and J. Lipkowski, *Acta Crystallogr., Sect. C: Cryst. Struct. Commun*., 2002, **58**, o683.

26 (*a*) R. D. Rogers and P. D. Richards, *J. Inclusion Phenom*., 1987, **5**, 631; (*b*) G. Weber, *J. Mol. Struct*., 1983, **98**, 333; (*c*) G. Weber, *Acta Crystallogr., Sect. C: Cryst. Struct. Commun*., 1983, **39**, 896; (*d*) B. L. Allwood, S. E. Fuller, P. C. Y. K. Ning, A. M. Z. Slawin, J. F. Stoddart and D. J. Williams, *J. Chem. Soc., Chem. Commun*., 1984, 1356; (*e*) J. A. Bandy, M. R. Truter and F. Vogtle, *Acta Crystallogr., Sect. B: Struct. Crystallogr. Cryst. Chem*., 1981, **37**, 1568; (*f*) R. D. Rogers, P. D. Richards and E. J. Voss, *J. Inclusion Phenom*., 1988, **6**, 65; (*g*) D. Henschel, K. Wijaya, O. Moers, A. Blaschette and P. G. Jones, *Z. Naturforsch., B: Chem. Sci*., 2000, **55**, 299; (*h*) A. Albert and D. Mootz, *Z. Naturforsch., B: Chem. Sci*., 1998, **53**, 242.

27 B. Piotrkowska, A. Wasilewska, M. Gdaniec and T. Polonski, *CrystEngComm*, 2008, **10**, 1421.

28 F. N. Allen, *Acta Crystallogr., Sect. B: Struct. Sci*., 2002, **58**, 380.

29 (*a*) Y. Levy and J. N. Onuchic, *Annu. Rev. Biophys. Biomol. Struct*., 2006, **35**, 389; (*b*) J. B. Pritchard and D. S. Miller, *Physiol. Rev*., 1993, **73**, 765; (*c*) P. L. Geissler, C. Dellago and D. Chandler, *J. Phys. Chem. B*, 1999, **103**, 3706.

30 (*a*) M. S. Fonari, V. Ch. Kravtsov, Yu. A. Simonov, S. S. Basok, E. V. Ganin, V. O. Gelmboldt, K. Suwinska, J. Lipkowski, O. A. Alekseeva and N. G. Furmanova, *Polyhedron*, 2008, **27**, 2049; (*b*) M. S. Fonari, Yu. A. Simonov, W.-J. Wang, S.-W. Tang, E. V. Ganin, V. O. Gelmboldt, T. S. Chernaya, O. A. Alekseeva and N. G. Furmanova, *Polyhedron*, 2007, **26**, 5193.

31 *COLLECT*, Nonius BV, Delft, The Netherlands, 1998.

32 Z. Otwinowski and W. Minor, in *Methods in Enzymology Macromolecular Crystallography, Part A*, ed. C. W. Carter and R. M. Sweet, Academic Press, London, 1996, vol. 276, p. 307.

33 G. M. Sheldrick, *SADABS*, Bruker AXS Inc., Madison, WI-53719, USA, 1997.

34 G. M. Sheldrick, *SHELXS97 and SHELXL97, Programs for Crystal Structure Solution and Refinement*, University of Göttingen, Germany, 1997.

35 C. F. Macrae, P. R. Edgington, P. McCabe, E. Pidcock, G. P. Shields, R. Taylor, M. Towler and J. van de Streek, *J. Appl. Crystallogr*., 2006, **39**, 453.

36 M. J. Frisch, G. W. Trucks, H. B. Schlegel, G. E. Scuseria, M. A. Robb, J. R. Cheeseman, J. A. Montgomery, Jr, T. Vreven, K. N. Kudin, J. C. Burant, J. M. Millam, S. S. Iyengar, J. Tomasi, V. Barone, B. Mennucci, M. Cossi, G. Scalmani, N. Rega, G. A. Petersson, H. Nakatsuji, M. Hada, M. Ehara, K. Toyota, R. Fukuda, J. Hasegawa, M. Ishida, T. Nakajima, Y. Honda, O. Kitao, H. Nakai, M. Klene, X. Li, J. E. Knox, H. P. Hratchian, J. B. Cross, C. Adamo, J. Jaramillo, R. Gomperts, R. E. Stratmann, O. Yazyev, A. J. Austin, R. Cammi, C. Pomelli, J. W. Ochterski, P. Y. Ayala, K. Morokuma, G. A. Voth, P. Salvador, J. J. Dannenberg, V. G. Zakrzewski, S. Dapprich, A. D. Daniels, M. C. Strain, O. Farkas, D. K. Malick, D. Rabuck, K. Raghavachari, J. B. Foresman, J. V. Ortiz, Q. Cui, A. G. Baboul, S. Clifford, J. Cioslowski, B. B. Stefanov, G. Liu, A. Liashenko, P. Piskorz, I. Komaromi, R. L. Martin, D. J. Fox, T. Keith, M. A. Al-Laham, C. Y. Peng, A. Nanayakkara, M. Challacombe, P. M. W. Gill, B. Johnson, W. Chen, M. W. Wong, C. Gonzalez and J. A. Pople, *GAUSSIAN 03 (Revision B.01)*, Gaussian, Inc., Pittsburgh, PA, 2003.

